Lasers in Manufacturing Conference 2017

Strain behavior during the initiation process of centerline cracks in laser welding of aluminum alloys

Christian Hagenlocher[a,*], Jonas Nolte[a], Rudolf Weber[a], Thomas Graf[a]

[a]*Institut für Strahlwerkzeuge, Universität Stuttgart, Pfaffenwaldring 43, 70569 Stuttgart, Germany*

Abstract

Welds in close edge position are affected by high transverse strains. These strains may lead to the formation of hot cracks. The spatial and temporal behavior of these strains was analyzed during laser welding by means of digital image correlation. In the experiments, MgSi alloyed aluminum sheets were joined by full penetration welding. Different welding parameters were investigated. The results show, that the temporal change of the strain (i.e. the strain rate) predicts the initiation of a centerline crack: A good agreement between the visible beginning of the centerline crack and the position of the change from negative to positive strain rates was determined.

Keywords: Laser welding; hot crack; digital image correlation; aluminum alloys;

1. Introduction

During solidification of aluminum alloys the grains are growing in the liquid melt within the temperature range between liquidus- and solidus temperature as stated by Borland, 1960 and Pellini, 1952. At the end of the solidification process, only thin films of liquid melt are remaining at the grain boundaries between the growing grains. In this condition, the solidifying material is very susceptible to mechanical loads. Prokhorov and Jakushin, 1968 called this range the Brittleness Temperature Range (BTR). If the mechanical load exceeds a critical value, the liquid film between the grains may tear, which results in hot cracks. Especially in laser beam welding in close edge position, inhomogeneous temperature distributions are present and high thermomechanical loads affect the weld. As welds offer a continuous grain boundary at their symmetry axis, continuous centerline cracks are well known defects in laser welding of aluminum alloys.

* Corresponding author. Tel.: +49 (0)711 685 66855; fax: +49 (0)711 685 66842.
E-mail address: christian.hagenlocher@ifsw.uni-stuttgart.de

Different theories exist, which kind of load causes hot cracks. According to Pellini, 1952 and Prokhorov and Jakushin, 1968 the acting strain causes hot cracks due to the low ductility within the BTR. Rappaz et al., 1999 and Cross, 2008 stated that the strain rate is the critical value for the initiation of a hot crack. According to the Model of Zacharia, 1994 hot cracks are caused by a critical stress which affects the solidification zone. Stritt, 2016 suggested a hot cracking criterion based on a critical crack energy, which is calculated by the values of stress and strain.

All those published criterions are based on critical mechanical values. In most cases the respective critical value is unknown, assumed or calculated, as it is difficult to measure strain or stress at high temperatures during solidification processes. Conventional tactile measurement technique, like strain gauges, are sensitive to temperature and limited to the determination of strain at one local point. However, to be able to predict the initiation of hot cracks one has to know this critical mechanical value.

In the present work digital image correlation was applied on high speed videos to measure the displacement in the immediate vicinity of the weld pool. This approach enables the experimental determination of strains and strain rates with a high temporal and spatial resolution during the formation of hot cracks. The value of critical mechanical loads can be experimentally identified by the results. It is shown that positive strain rate is required for inducing a hot crack and that the change of strain rate from negative to positive values serves as an indicator for the prediction of the initiation of hot cracks.

2. Experimental Setup

Fig. 1 sketches the experimental setup. It is based on the Setup presented by Hagenlocher et al., 2016. The laser beam moves in positive *x*-direction with the feed rate v_s, whereas the sample and high speed camera remained stationary. Thus, the high speed camera recorded videos of a field of view (FOV) at a stationary *x*-position on the sample. To observe the strain behavior at different weld progresses (i.e. *x*-positions), the clamping device was adjustable in *x*-direction (see Fig. 1).

To avoid distortions of the image, caused by the angle of view, the high speed camera was orientated perpendicular to the surface of the sample. A diode laser with a wavelength of 809 nm illuminated the FOV. An appropriate band pass filter was integrated in the optical path of the high speed camera. The FOV had a size of 20 x 15 mm² which led to a projected scale of more than 100 px/mm with the resolution of the camera chip of 1600x1200 px². The framerate was 1 kHz.

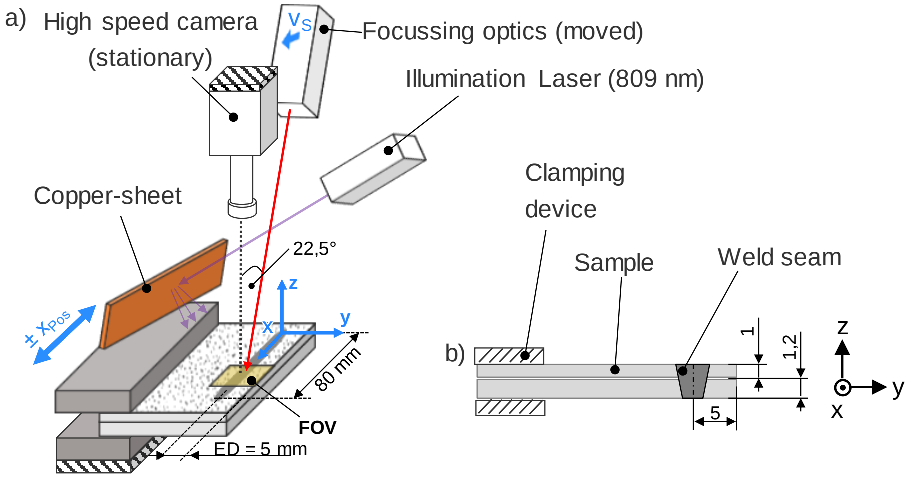

Fig. 1. (a) Sketch of experimental setup; (b) geometrical dimensions of the sample

A disk laser Trudisk16002 was used to join two aluminum sheets (AA6541) with a thickness of s_1 = 1 mm and s_2 = 1.2 mm in overlap configuration, as shown in Figure Fig. 1b. All welds were full penetration welds performed at an edge distance of 5 mm to create a high thermomechanical tensile load during the welding process, aiming at the formation of centerline cracks. The laser parameters and focusing conditions were kept constant throughout the experiments and are listed in Table 1.

Table 1. Laser parameters and focusing conditions.

Parameter	Value
Core diameter of fiber	200 µm
Focal length collimation lens	200 mm
Focal length focusing lens	560 mm
Focal diameter on the surface of the sample	560 µm
Rayleigh length	7.84 mm
M^2	30.5
Wavelength of laser beam	1.03 µm
Shielding gas	N_2

The feed rate and the laser power were varied and the investigated parameter sets are listed in Table 2. High speed videos were recorded at different x-positions for each parameter set.

Table 2. Welding parameters.

Feed rate	Laser power
4 m/min	4 kW
6 m/min	5 kW
9 m/min	7 kW

3. Method

Fig. 2 describes the three steps of strain determination. A stochastic black and white pattern was applied on the surface of the sample by spraying, prior to the experiments. The applied paint is resistant to temperatures below the melting temperature of aluminum alloys. Then a high speed video of the process is recorded during the process.

The second step is the analysis of the high speed videos by digital image correlation. Digital image correlation algorithms track the movements of the grey-scale gradients of the applied pattern. The results are the time-resolved local displacements of the pattern (i.e. the surface of the sample) in Micrometers as illustrated by the color-mapped total displacement after the process in *y*-direction in the top middle of Fig. 2.

The strain, which affected the weld in transverse direction, was determined by the measured displacements as presented by Hagenlocher et al., 2016. Different displacements of two given points lead to a change of their distance. This change of distance is expressed by the engineering strain ε in the following. In the present work only the transverse strain ε_y is regarded (yellow arrow in the center of the image top middle of Fig. 2). Especially the temporal evolution of the transverse strains ε_y at a respective *x*-position (as shown in the top right image of Fig. 2) is analyzed in the following.

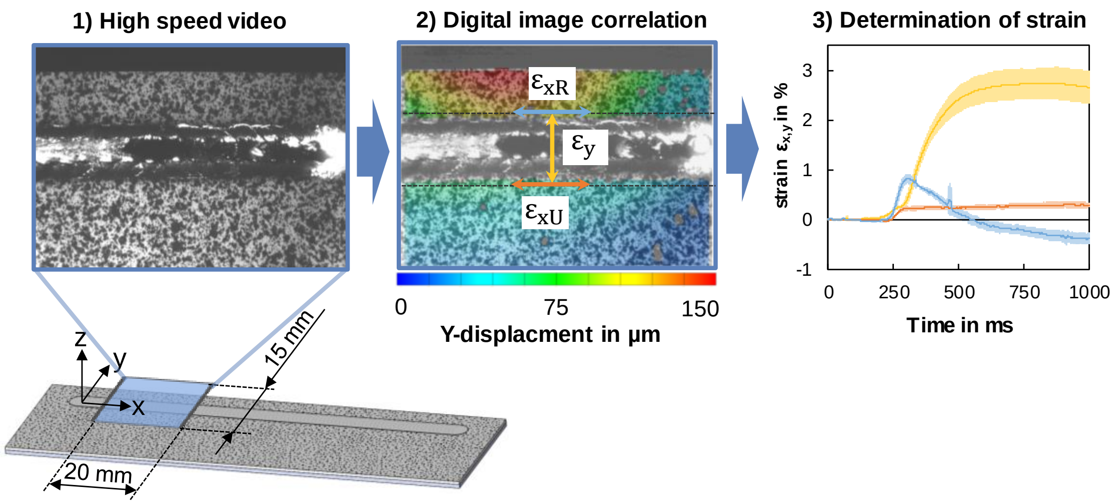

Fig. 2. Procedure of the determination of the time resolved transverse strain.

4. Results

4.1. Position of crack initiation

The position of the crack initiation was determined first, to be able to evaluate the strain and strain rates in the vicinity of this point. Fig. 3 shows microscope images of the surface of weld seams for different process parameters in the area of the beginning of the centerline crack. The colored bars of the diagram indicate the averaged *x*-position of the beginning of the crack of 5 analyzed weld seams. The error bars show the standard deviation of the measured values. Crack initiation occurred earlier in case of welding with higher laser power and feed rate.

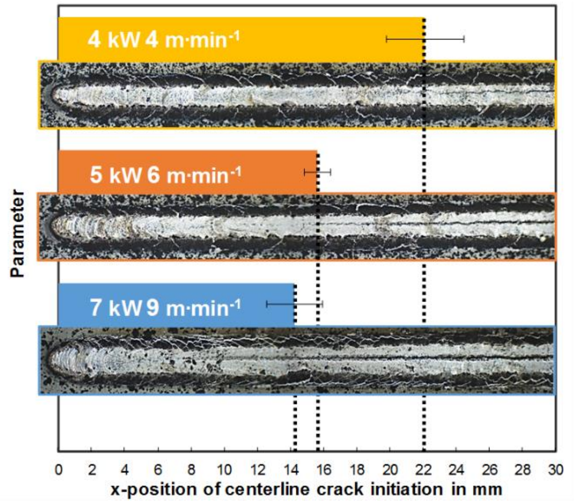

Fig. 3. Visible beginning of centerline cracks in weld seams of different process parameters.

4.2. Strain at hot crack initiation

One required condition for the occurrence of hot cracks is a positive transverse strain at the solidification zone. The end of the weld pool indicates the beginning of the solidification zone and can be determined from the high speed videos. As a stationary *FOV* was observed, the end of the weld pool passed different *x*-positions at different times. Fig. 4 shows the transverse strain of welding with a laser power of 5 kW and a feed rate of 6 m/min as a function of time at different x-positions. In the top of Fig. 4 the resulting weld seam is sketched including the beginning of the centerline crack at 16.3 mm (compare Fig. 3). The points in time, at which the weld pool passes the respective *x*-position are marked with blue dots.

It can be seen, that the strain which is affecting the weld is increasing with increasing *x*-position (i.e. weld progress). At the beginning of the weld ($x < 12$ mm) it changes from negative (i.e. compressive strain) to positive (i.e. tensile strain) values. The initiation of the crack occurred when the tensile strain at the beginning of the solidification zone exceeded a critical value of $\varepsilon_y > 1$ %.

At the *x*-position, where no centerline crack was present ($x = 8$ mm and $x = 12$mm), the strain decreased, after the end of the weld pool passed the respective *x*-position. At positions where a centerline crack was present ($x = 20$ mm and $x = 24$ mm) the strain increased after the crack was initiated.

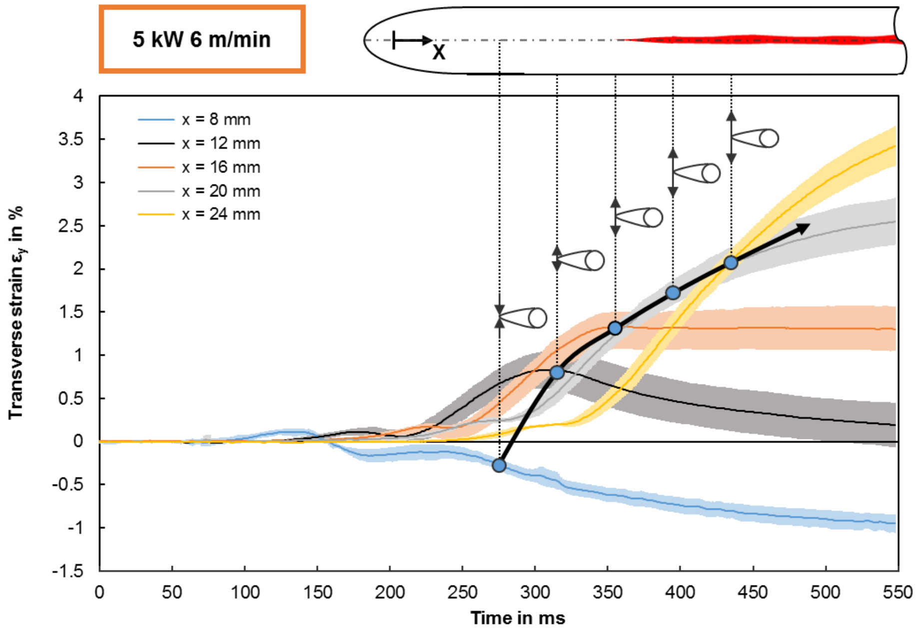

Fig. 4. Transverse strains as function of time at different x-positions in the area of crack initiation in case of welding with a laser power of 5kW and a feed rate of 6 m/min (Data points of strain at the weld pool's end are marked with blue dots).

Fig. 5 shows the averaged transverse strain (blue dots in Fig. 4) at the end of the weld pool as a function of *x*. The colors of the curves refer to different process parameters. The error bars indicate the standard deviation of five measurements. The strain values and *x*-positions of crack initiation are marked with dotted black lines.

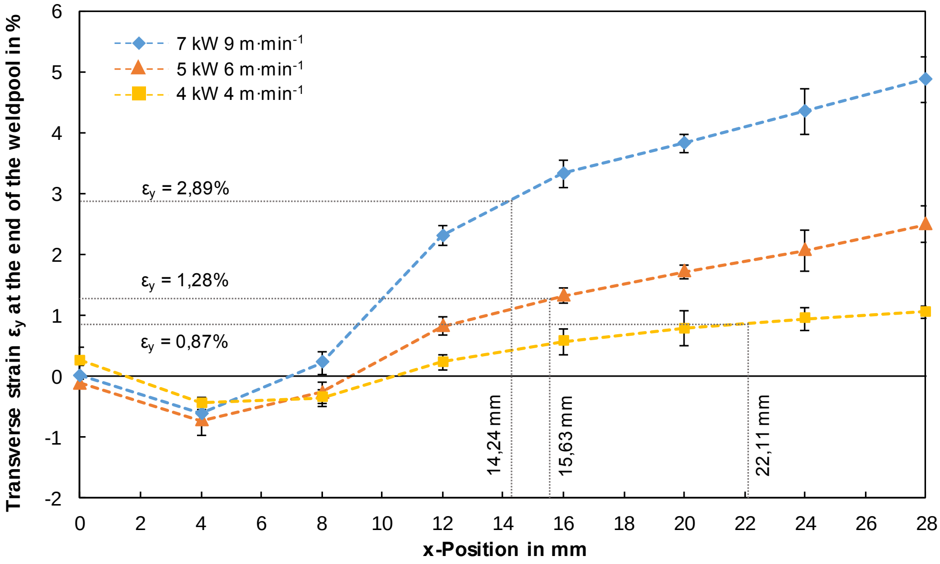

Fig. 5. Transverse strain at the end of the weld pool during hot crack initiation for different process parameters.

At the different *x*-positions of crack initiation, different values of strain affected the end of the weld pool, i.e. the solidification zone: The value of the strain, which affected the solidification zone, increased with increasing laser power and feed rate.

4.3. Strain rate at hot crack initiation

Fig. 6 shows the averaged transverse strain rate, $\dot{\varepsilon}_y$, at the end of the weld pool as a function of *x*. The strain rate is the temporal derivation of the strain. The colors of the curves refer to different process parameters. The error bars indicate the standard deviation of five measurements. The *x*-positions of crack initiation are marked with vertical lines.

Again higher values were determined in case of higher laser power and feed rate. Fig. 6 shows, that also a positive strain rate value must be present for the initiation of a centerline crack. Moreover, the change from negative (i.e. compressive) to positive (i.e. tensile) strain rate values predicts the initiation of centerline crack within the next 3 mm of welding route.

A comparison of the yellow curves of Fig. 5 and Fig. 6 gives evidence that both, a positive strain and strain rate, are necessary for the initiation of a hot crack. Though positive total strains (Fig. 5) were present at the end of the weld pool between x ≈ 10 mm and x ≈ 20 mm negative strain rates (Fig. 6) avoided the hot crack initiation.

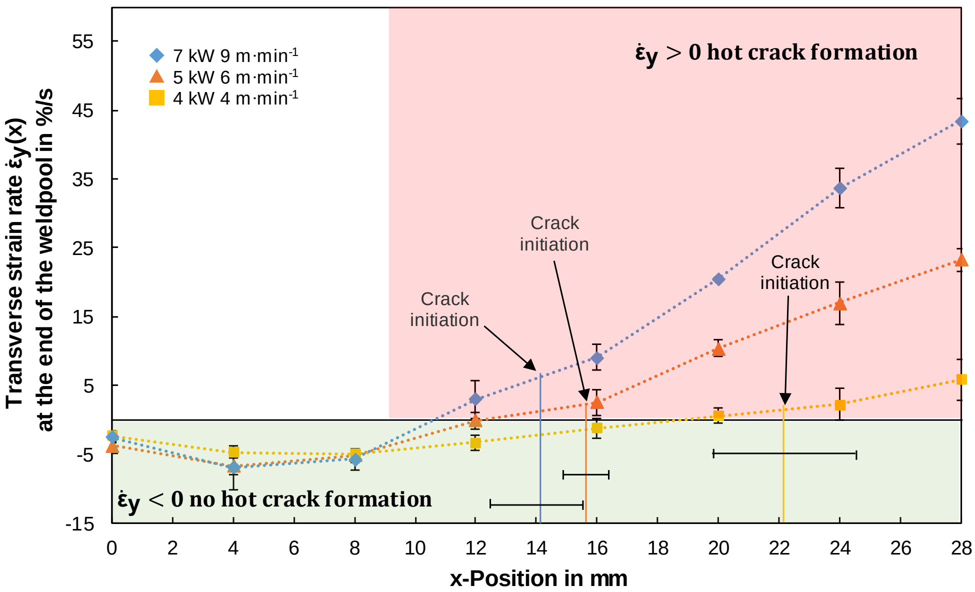

Fig. 6. Transverse strain at the end of the weld pool during hot crack initiation for different process parameters.

5. Conclusion

Thermomechanical strains and strain rates during laser beam welding were determined by means of digital image correlation. The results show that higher laser power and feed rate lead to higher strain rate and strain values during the welding process and to higher positive (i.e. tensile) strains, which are affecting the solidification zone during hot crack initiation. However, both, a positive strain and strain rate at the solidification zone are required for the initiation of a centerline hot crack. The change of the strain rate from negative (i.e. compressive) to positive (i.e. tensile) values predicts the initiation of a centerline crack and offers the possibility to proof weld seams in process or even control the process.

References

Borland, J. C., 1960. Generalized theory of super solidus cracking in welds (and castings), Brit. Welding Journal No.7, p. 508

Cross, C. E., 2008. Weld Solidification Cracking: Critical Conditions for Crack Initiation and Growth, Berlin, Springer Verlag (Hot Cracking Phenomena in Welds II), p. 39

Hagenlocher, C.; Stritt, P.; Friebe, H.; Blumenthal, C.; Weber, R.; Graf, T., 2016. Space and time resolved determination of thermomechanical deformation adjacent to the solidification zone during hot crack formation in laser welding., Proc. of ICALEO'16

Pellini, W. S., 1952. Strain Theory of Hot Tearing, Foundry No.80, p. 125

Prokhorov, N. N.; Jakushin, B. F., 1968. Theorie und Verfahren zur Bestimmung der technologischen Festigkeit von Metallen während des Kristallisationsprozesses beim Schweißen, Schweißtechnik Nr.18, p. 8

Rappaz, M.; Drezet, J.-M.; Germaud, M., 1999. A New Hot-Tearing Criterion, Metallurgical and Materials A vol.30A, p. 449

Stritt, P., 2016. Prozessstrategien zur Vermeidung von Heißrissen beim Remote-Laserstrahlschweißen von AlMgSi 6016. Dissertation. Universität Stuttgart, Stuttgart. Inst. f. Strahlwerkzeuge

Stritt, P.; Hagenlocher, C.; Weber, R.; Graf, T., 2016. The effect of Laser welding parameters on the grain structure distribution in the resultant weld, Proc. of ICALEO'16

Zacharia, T., 1994. Dynamic stresses in weld metal hot cracking, Welding Journal Vol.73 No.7, p. 164